Available online at www.sciencedirect.com

ScienceDirect

Procedia Materials Science 8 (2015) 665 – 673

Procedia Materials Science

www.elsevier.com/locate/procedia

International Congress of Science and Technology of Metallurgy and Materials, SAM - CONAMET 2013

Photothermal Microscopy

Facundo Zaldivar Escola[a], DaríoKunik[b], Oscar Eduardo Martinez[a], Nélida Mingolo[a,*]

[a]*Universidad de Buenos Aires, Facultad de Ingeniería, Paseo Colon 850, 1063 Buenos Aires, Argentina*
[b] *Tolket S.R.L, Int., Güiraldes 2160, Pabellón I, Cdad. Universitaria, CABA C1428EAH, Argentina*

Abstract

An accessory for a commercial optical microscope was implemented to map the thermal diffusivity of the sample with high spatial resolution. The system is based in the photothermal technique recently developed by the group. It consists in the measurement with a probe laser of the surface curvature induced by the heat delivered by a modulated pump laser. A lock-in detection technique provides the signal amplitude and phase as a function of the modulation frequency. The accessory was mounted on the camera port of a metallographic microscope Olympus BX51. Results obtained on different samples are presented.

Selection and peer-review under responsibility of the scientific committee of SAM - CONAMET 2013

Keywords: thermal diffusivity; photothermal; microscopy.

1. Introduction

The use of a modulated or pulsed laser beam to heat a sample to produce thermal waves was introduced in the 1980's. In the last few decades several related techniques have been developed, such as those based in the infrared emission of the heated surface (IR radiometry), Nordal (1979), Busse (1980), the deflection of a grazing beam by mirage effect, Salazar (1991), or deflection due to surface deformation (photothermal deflection), Rosencwaig (1983), Opsal (1983), the change in the reflectivity with temperature, probed with a second laser (thermoreflectance), Rosencwaig (1985). Some of this techniques have been used for the microscopic

* Corresponding author.
*E-mail address:*nmingol@fi.uba.ar

Selection and peer-review under responsibility of the scientific committee of SAM - CONAMET 2013
doi:10.1016/j.mspro.2015.04.123

determination of the thermal diffusivity and the two dimensional mapping of thermal properties. The IR radiometry has been extensively used for depth profiling, Ma (1992), Munidasa (1998), Celorrio (2010), Glorieux (1999), but it has limitations in the lateral resolution, Bisson (1998), due to the use of IR wavelength in the detection process. Thermoreflectance has been used successfully for microscopic evaluations, Bincheng (1999), Fournier (2001), Rochais (2005), but requires the independent scan of the two beams (pump and probe) to measure the phase delay as a function of the distance between the beams or else a frequency scan at fixed relative positions of the beams requiring a very precise pointing stability. The technique depends in the variation of the reflectivity of the probe beam with the temperature of the sample, information not readily available for different materials and a parameter that can change significantly with the different phases of the same material to be mapped with microscopic resolution. The photodeflection method has been successfully used for microstructure mapping, Crossa (2010), and even mapping the hardness of treated steels, Crossa (2011), but the setup requires stringent and severely limitant pointing stability, Martinez (2008).

In a recent work, Mingolo (2012), a new photothermal technique was introduced, based in the measurement of the curvature induced by the thermal expansion of the material, sensed with a probe beam collinear with the heating pump beam. To ensure the colinearity of the two beams the lasers were combined in a single mode fiber using telecom technology. The laser wavelengths were in the near IR, which complicates adding them to a conventional microscope due to the need of special optics for that wavelength.

In this work a new development is introduced that makes use of visible semiconductor lasers that are combined in a similar manner as before with the IR telecom devices and is added to a commercial microscope through standard camera ports. The accessory includes two galvanometric scanners to sweep the beams over the surface of the sample and map the thermal diffusivity with micrometric resolution.

2. Experimental

The method is illustrated in figure 1. A single fiber delivers the pump and probe lasers, that are collimated by a lens of focal distance f1 and are focused on the surface by a lens of focal length f2. As the pump laser is modulated at a frequency f, the surface expands and contracts at that same frequency, with an amplitude and phase that depends on the beam size and the thermal diffusivity of the sample, Mingolo (2012). A probe laser is reflected on the sample surface (that must be polished) and is collected back with the same optical fiber. The sample is not located exactly at the focal plane but instead it is defocused by an amount δ. Upon reflection in a thermally expanded curved surface the beam is focused in the return path at a distance δ' from the fiber tip. As δ' depends on the thermal expansion (curvature) it oscillates at the pump modulating frequency. The collected fraction of the probe beam varies in time with an amplitude that depends in Q, the inverse of the surface radius of curvature R=1/Q. There is another mechanism appearing that introduces a variation in the collected power and it is the change in reflectivity with temperature (thermoreflectance).

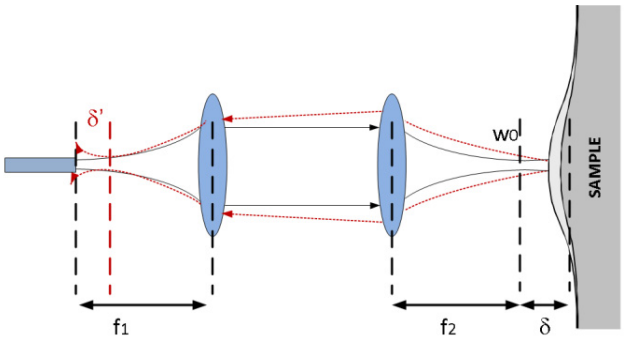

Fig. 1. Schematics of the working principle of the technique. As the pump heats the sample and it expands, the probe beam is defocused and its reinjection into the fiber changes.

The collected signal results, Mingolo (2012):

$$S_\omega = \alpha f(\omega/\omega_0) + \beta h(\omega/\omega_0) \tag{1}$$

where α and β are real coefficients that depend on the power of the lasers and properties of the material, Mingolo (2012), ω is the modulation frequency and

$$\omega_o = \frac{2D}{\sigma^2} \tag{2}$$

is a critical frequency that depends on the thermal diffusivity in the impinging location and σ is the radius of the Gaussian pump beam defined as the distance where the intensity decays by 1/√e. The functions *f* and *h* are complex and given by:

$$f(\omega/\omega_o) = \int_0^\infty \frac{e^{-u}}{\left(u + i\frac{\omega}{\omega_o}\right)^{\frac{1}{2}}} du$$
$$h(\omega/\omega_0) = \int_0^\infty \frac{e^{-u}u}{(u + i\omega/\omega_0)} du \tag{3}$$

The amplitude and phase of these functions is plotted in figure 2.

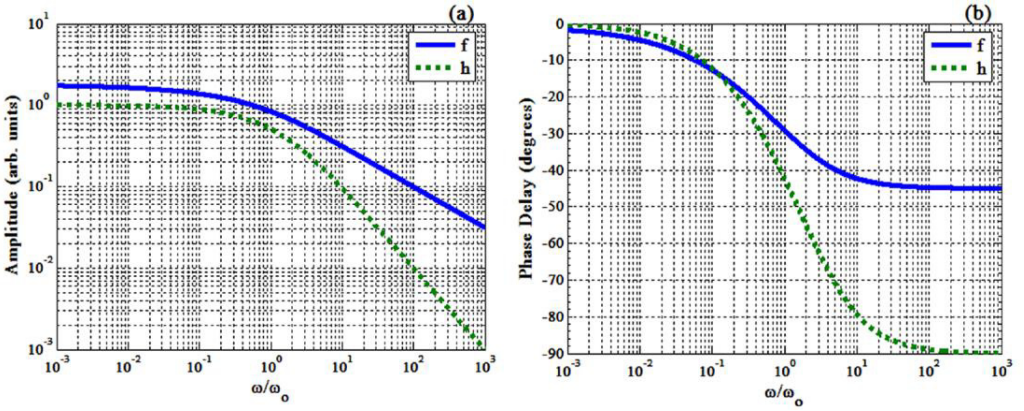

Fig. 2. Theoretical curves for the contributions in amplitude and phase delay of the thermoreflectance (*f*) and the expansion (*h*).

From the numerical fit of the experimental data with equation (1) the parameters α and β are retrieved as well as the critical frequency ω_0. The ratio between α and β indicates the relative relevance of both mechanisms involved (thermal expansion and thermoreflectance).

In figure 3 a schematic of the layout is shown. A semiconductor laser emitting at 660nm is used as a pump source and another one at 785nm is used as probe. Both lasers are monitored taking samples from 1% couplers, and then combined in a single fiber by a wavelength division multiplexer (WDM). The return probe beam is directed towards a detector coupled to a lock-in amplifier that provides the amplitude and phase delay of the signal at the modulation frequency. Figure 4 shows a picture of the equipment and a schematic of the scanning and focusing optics. A pair of galvanometric mirrors scans the beams on a plane that is projected to the surface of the sample. The system is coupled to an Olympus BX51 microscope through a lateral camera port. A second camera port provides an image of the sample surface and the software is used to select within that image the region to be scanned.

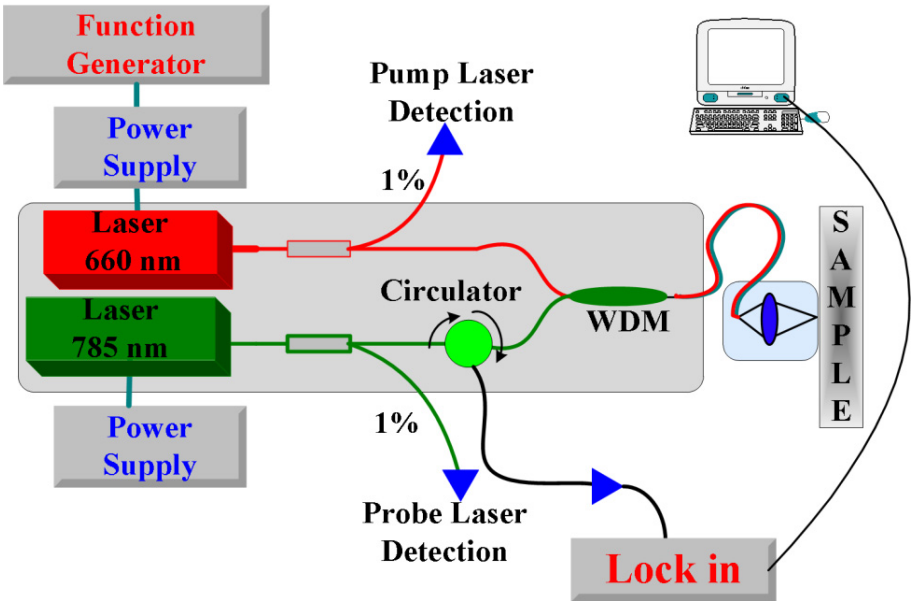

Fig. 3.Schematics of the device.

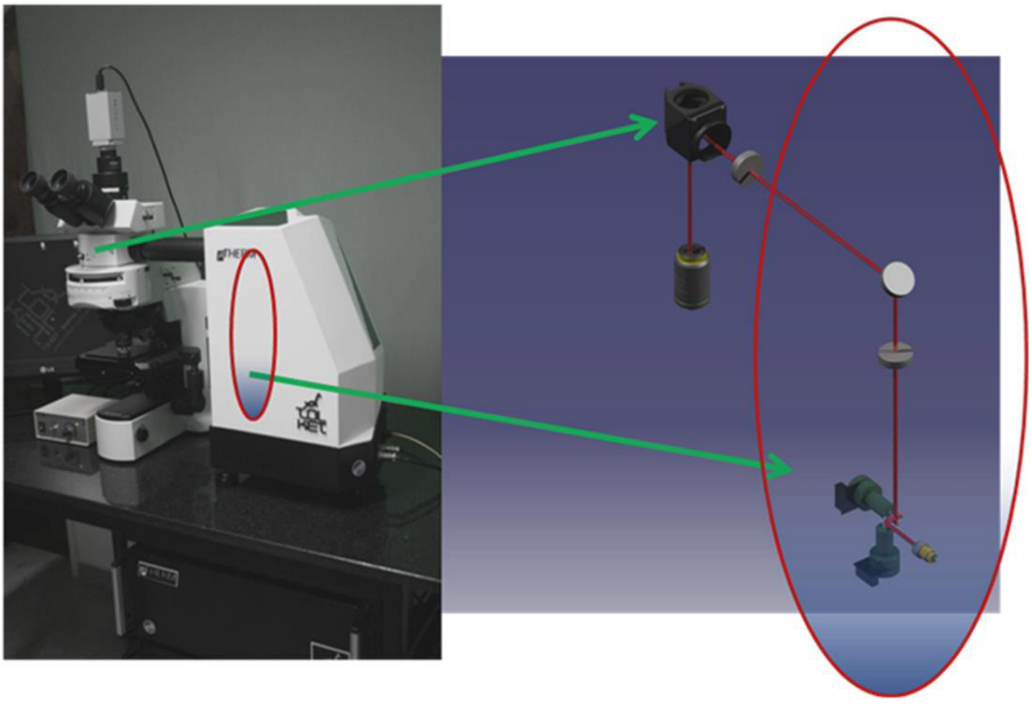

Fig. 4. Photograph of the equipment attached to the microscope and schematics of the ray paths through the galvanometric mirrors and the corresponding optics.

3. Results and discussions

To test the system we selected the same sample studied before with the photodeflection technique, Zaldivar (2013), consisting in a sintered pellet of oxides of Uranium and Gadolinium. These mixed oxides are used as nuclear fuels and it is relevant to determine the homogeneity, the presence of clusters not inter-diffused and if the oxides are just finely mixed or have actually inter-diffused. The measurement of the thermal diffusivity is particularly suitable for this purpose because Gadolinea has a thermal diffusivity 4 times larger than Urania, but when Gadolinium diffuses as impurity in the Urania lattice the thermal diffusivity decreases, Zaldivar (2013).As the band gap of Urania is close to the photon energy of the pump laser, a thin Pt coating (20nm) was added to act as absorption layer. Platinum absorbs 20% of the incoming power, reflecting the other 80%, providing a thin layer that transmits the heat towards the substrate. The layer is thin enough that the lateral heat conduction within the Pt layer can be neglected Domené (2009).

It has been shown, Crossa (2010), that if the thermoreflectance is negligible the map of the thermal diffusivity can be retrieved with a single measurement per point at a fixed modulation frequency. To check if this was the case with the Pt layer and the probe wavelength used, a frequency scan was performed at a fixed point and the result fit by equation (1). The contribution to the thermoreflectance comes only from the coating, while the thermal expansion contribution is mainly from the substrate, because the coating is too thin to contribute significantly to the expansion. In figure 5 the amplitude and phase of the signal obtained at an arbitrary point of the sample is plotted together with the fit obtained with equation (1). The separate contributions to the fit of the term proportional to $f(\omega/\omega_0)$ and $h(\omega/\omega_0)$ are also shown. From the fit a relation $\beta/\alpha=26.6$ is obtained indicating that the dominant contribution comes from the expansion mechanism. The value of $D= (0{,}0287 \pm 0{,}0015)\text{cm}^2/\text{s}$ obtained is consistent with Urania with interdiffused Ga impurities, Zaldivar (2013).

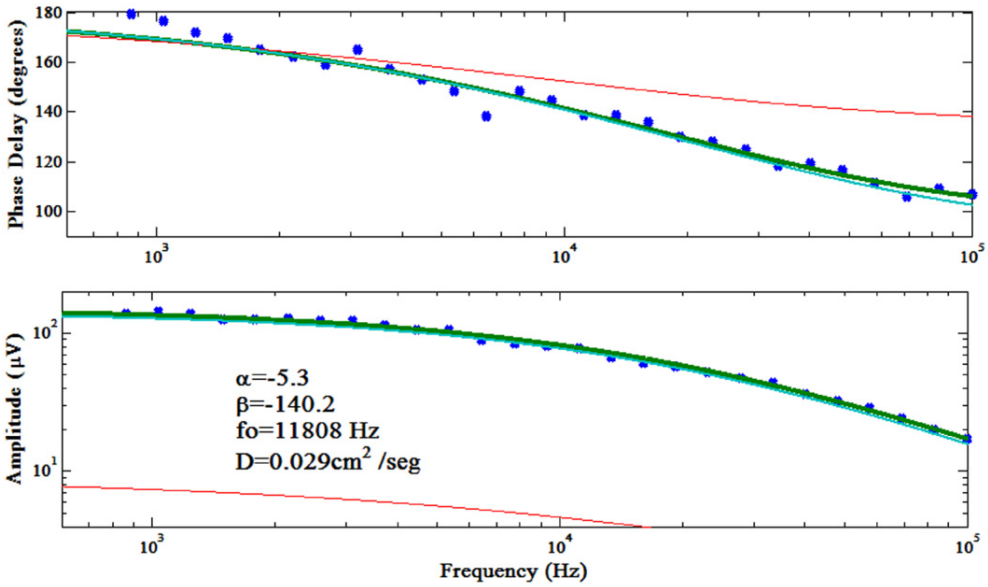

Fig. 5. Plots of the frequency scan at a fixed location and fit to the theoretical expression.

The fact that the thermoreflectance contribution is negligible allows the retrieval of the thermal diffusivity by scanning the surface at a constant modulation frequency (close to the critical frequency), and from the plot of the phase delay of figure 2 the critical frequency can be computed using the curve for the function *h*.

As the critical frequency obtained with the frequency scan was 11.8kHz, a frequency f=10kHz was chosen for the scans. In figure 6 the image obtained with the microscope camera is presented and the box indicates the region scanned. The figure in the right corresponds to the image provided by the map of the reinjected CW amplitude at each point (reflectivity map). The amplitude and phase delay at the modulation frequency is presented in figure 7.

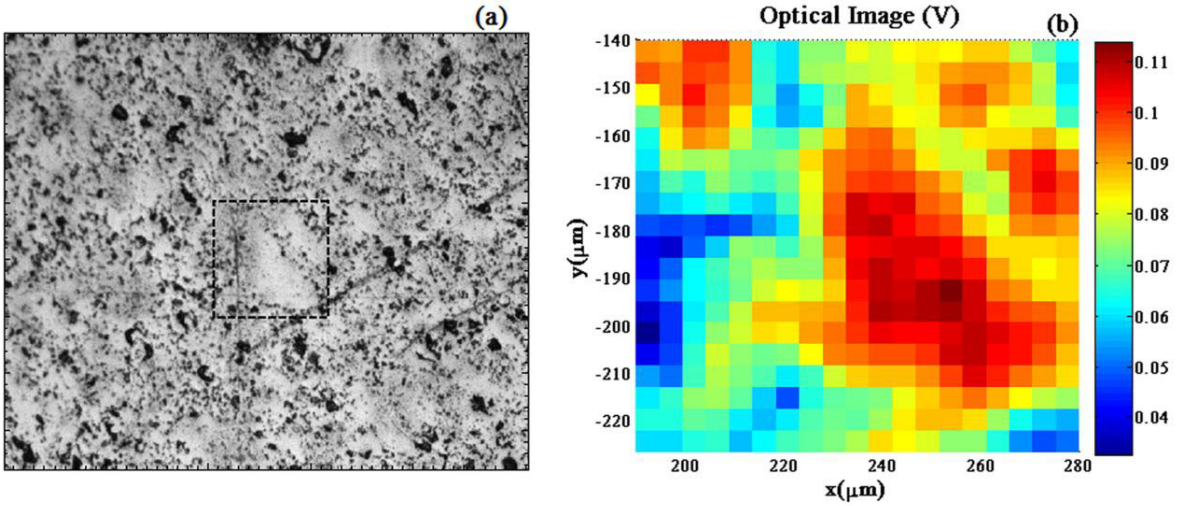

Fig. 6. (a): Image obtained with a CCD camera. The box indicates the scanned region.(b) Optical scan with the equipment in the same region.

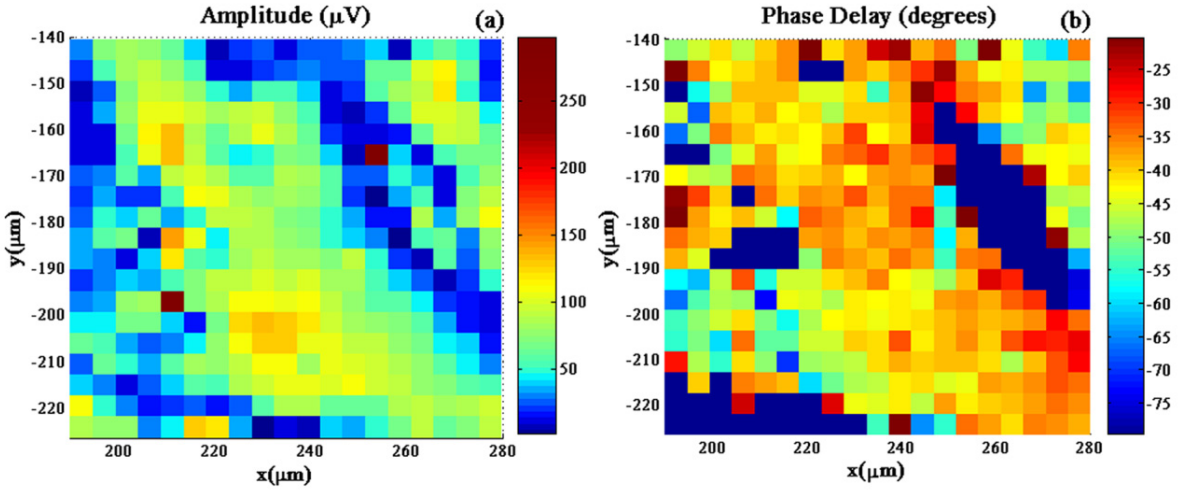

Fig. 7. Amplitude (a) and phase delay (b) as a function of the position in the sample.

As mentioned before, from the phase delay as a function of the normalized frequency the thermal diffusivity can be retrieved. To do this the phase of the complex function *h* is inverted and plotted in figure 8, where:

$$\frac{D}{D'} = \frac{f_0}{f} = \frac{D}{\pi\sigma^2 f} \tag{4}$$

From the plot it can be noticed that there is a linear region (in semilog scale) for which the following sensitivity is obtained:

$$\frac{\Delta D}{D} = 5{,}9\frac{\%}{\text{Degree}} \tag{5}$$

which indicates that regions with a shift in the phase delay of 1 degree will have a relative difference in the thermal diffusivity of 5.9%. It is worthwhile mentioning that when this same procedure is carried out in a photodeflection experiment, the curve to be used to convert phase delay into thermal diffusivity depends on the relative separation between the pump and probe beams, which forces a calibration for each measurement. With the technique presented here the conversion curve of figure 8 is universal and does not change with the experiment or equipment used.

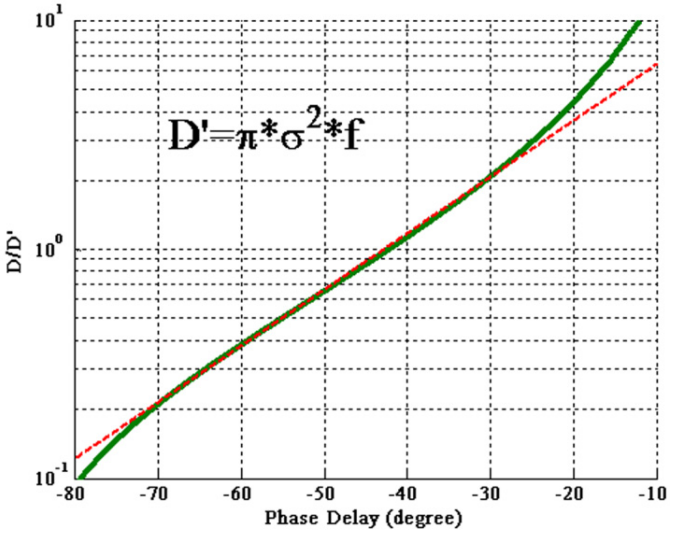

Fig. 8. Conversion curve from phase delay to thermal diffusivity. The dotted line is a guide to the eye to notice the linearity in the central region.

In order to determine the precision of the technique and verify that the changes in the thermal diffusivity presented in the map of figure 7 correspond to actual changes in the diffusivity, a map on a homogeneous sample was performed. The sample chosen was a fused silica substrate coated with a Pt thin film similar to that of the previous experiment. In figure 9 the histograms of the phase delay maps for the Urania/Gadolinea mixture and fused silica samples are presented. Both histograms were fitted with Gaussians and from the width of the fused silica histogram it can be stated that the precision of the method in determining the thermal diffusivity at the scanning speed used is better than 5%. The scanning speed was the same for both maps. The integration time for each point on the map was 1 second, and the program waited 10 seconds before the point was changed, to ensure the stability of the measurement. For each map, the time elapsed was 1 hour (approximately). It is worthwhile mentioning that from equation (2), if σ (the radius of the Gaussian pump beam) is reduced, the critical frequency ω_0 will grow and a larger frequency for the scans can be chosen. This increment in the frequency scan allows the reduction of the integration time resulting in faster measurements or alternatively in a better resolution with the same scanning time.

In figure 10 the map of thermal diffusivity for the scan shown in figure 7, and converted using the curve of figure 8, is presented together with its corresponding histogram. The dark blue regions of zero thermal diffusivity correspond to regions with pores where the signal is null. These points were not included in the histogram. The average value obtained for the thermal diffusivity in the scanned region was 0.025cm^2/s, consistent with the expected value for Urania with Ga impurities and the standard deviation of 0.009cm^2/s is an indication of the homogeneity of the sample. Within this range fall the value for pure Urania (D=0.033cm^2/s) and for UO_2-10%GdO_3 (D=0.0156 cm^2/s), Zaldivar (2013).

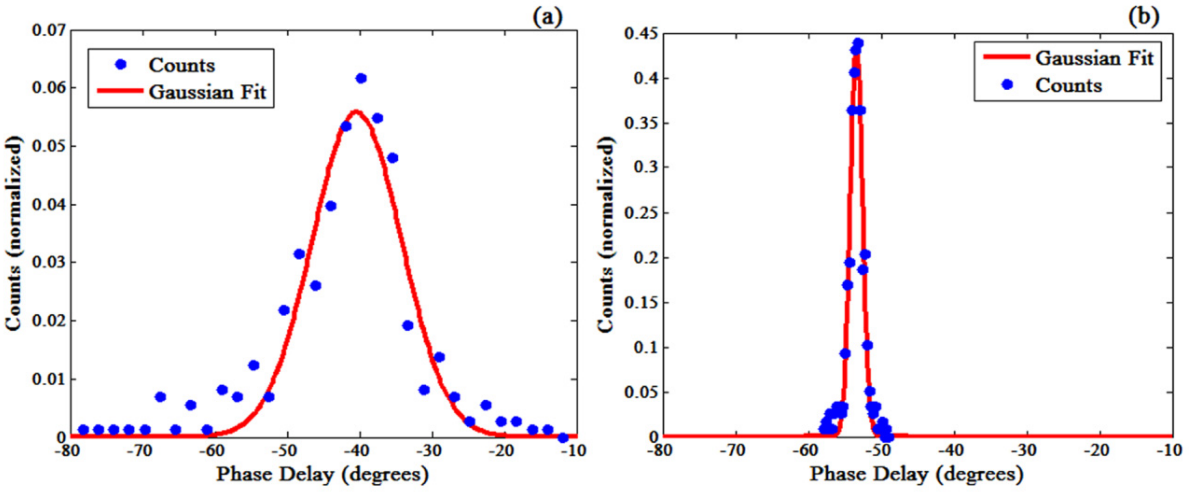

Fig. 9. Histograms obtained from the maps of phase delay of the (a) oxide mixture (width:5.9º) and (b) SiO2 (widht: 0.9º). Full lines: Gaussian fit to the histograms.

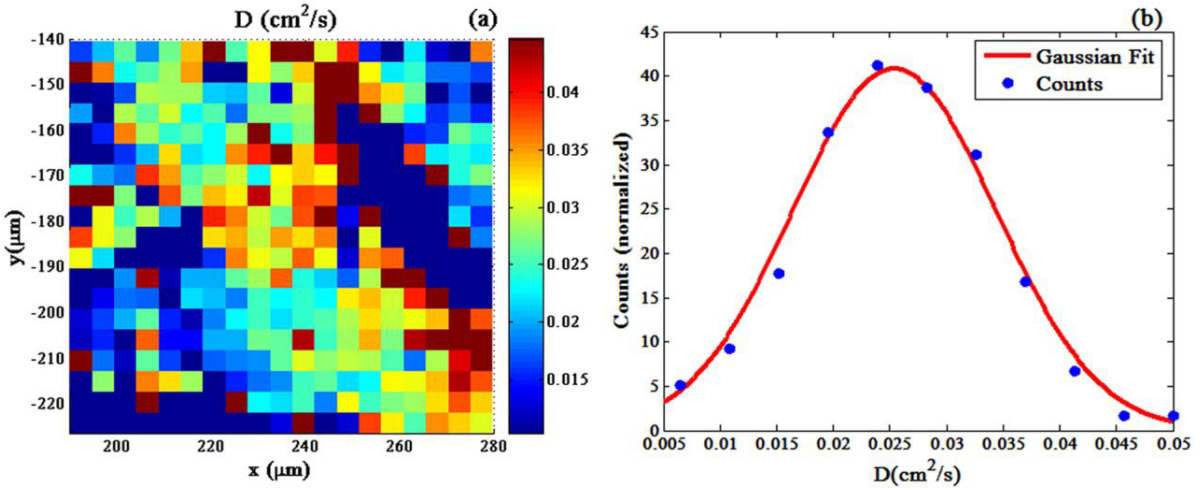

Fig. 10. (a) Diffusivity map of the mixed oxide simple; (b) Histogram of the map and Gaussian fit.

4. Conclusion

An accessory for commercial microscopes has been developed that provides a map of the thermal diffusivity of materials at a microscopic level with a precision of 5%. The system was build with optical fiber components similar to those used in optical communications but working in the visible range to easily adapt it to commercial microscopes. The system includes a pair of galvanometric mirrors to scan the beams on the sample to create an image. A CCD camera is also included to visualize the region to be scanned prior to start the measurement. The software developed allows the modulating frequency scan to increase the accuracy of the retrieved values at selected points.

It was shown that a thin Pt layer (a few tens of nm) is suitable as an absorption layer that transmits the heat to the substrate without introducing a significant thermoreflectance signal at the wavelength of 785nm used as probe. This fact allows a scan at constant modulation frequency to map the thermal diffusivity, indicating that its use would be convenient even in the case of opaque materials (such as metals).

Finally the results obtained with a sample of mixed oxides used for nuclear fuels were presented. A map of thermal diffusivity was shown that allows to determine the homogeneity of the material, the detection of the presence of clusters of material that did not mix and also if the minority material (Ga in our case) is adequately inter-diffused. This is possible because when an impurity diffuses the heat transport by phonons decreases and hence also decreases the thermal diffusivity. Conversely if the oxides are simply mixed, an intermediate thermal diffusivity between the two components would be found, that in this case would be higher than that of pure Urania (the majority oxide).

Acknowledgements

The authors wish to acknowledge grants from UBACyT.

References

Bincheng Li, Roger J. P., Pottier L., Fournier D., 1999. Complete thermal characterization of film-on-substrate system by modulated thermoreflectance microscopy and multiparameter fitting. Journal of Applied Physics. 86, 5314-5316.

Bisson J.F. Fournier D., 1998. Application of infrared microscopy to thermal diffusivity measurement in refractories at various temperatures. High temperatures-high pressures 30, 205-210.

Busse G., 1980. Photothermal transmission probing of a metal. Infrared Phys. 20, 419-422.

Celorrio R., Apiñaniz E., Mendioroz A., Salazar A., Mandelis A., 2010. Accurate reconstruction of the thermal conductivity depth profile in case hardened steel. Journal of Applied Physics. 107, 083519.

Crossa Archiopoli U., Mingolo N., Martínez O. E., 2010. Two-dimensional imaging of thermal diffusivity in metals by scanning photodeflection detection. Journal of Applied Physics 107, 023520.

Crossa Archiopoli U., Mingolo N., Martínez O. E., 2011. Two-dimensional mapping of micro-hardness increase on surface treated steel determined by photothermal deflection microscopy. Surface and Coatings Technology 205, 3087-3092.

Domené E. A., Balzarotti F., Bragas A. V., Martínez O. E., 2009. Photothermal measurement of absorption and scattering. Losses in thin films excited by surface plasmons. Optics Letters 34, 3797-3799.

Fournier D. 2001. Thermal-Wave Probing at Various Spatial Scales. MRS Bulletin, Jun2 2001, 465-470.

Glorieux C., Li Voti R., Thoen J., Bertolotti M., Sibilia C., 1999. Depth profiling of thermally inhomogeneous materials by neural network recognition of photothermal time domain data. Journal of Applied Physics 85, 7059-7063.

Ma T. C., Munidasa M., Mandelis A., 1992. Photoacoustic frequency-domain depth profilometry of surface-layer inhomogeneities: Application to laser processed steels. Journal of Applied Physics 71, 6029-6035.

Martínez O. E.,Balzarotti F., Mingolo N., 2008. Thermoreflectance and photodeflection combined for microscopic characterization of metallic surfaces. Applied Physics B: Lasers and Optics 90, 69-77.

Mingolo N., Martínez O. E., 2012. Focus shift photothermal method for thermal diffusivity mapping. Journal of Applied Physics. 111, 123526.

Munidasa M., Funak F., Mandelis A., 1998. Application of a generalized methodology for quantitative thermal diffusivity depth profile reconstruction in manufactured inhomogeneous steel-based materials. Journal of Applied Physics. 83, 3495-3498.

Nordal P. E., Kanstad S. O., 1979. Photothermal Radiometry. Physica Scripta 20, 659-662.

Opsal J., Rosencwaig A., Willenborg D. L., 1983. Thermal-wave detection and thin-film thickness measurements with laser beam deflection. Applied Optics 22, 3169-3176.

Rochais D., Le Houëdec H., Enguehard F., Jumel J., Lepoutre F., 2005. Microscale thermal characterization at temperatures up to 1000°C by photoreflectance microscopy. Application to the characterization of carbon fibres. J. Phys. D: Appl. Phys. 38, 1498-1503.

Rosencwaig A., Opsal J., Willenborg D. L., 1983. Thin-film thickness measurements with thermal waves. Appl. Phys. Lett. 43, 166-168.

Rosencwaig A., Opsal J., Smith W. L., Willenborg D. L., 1985. Detection of thermal waves through optical reflectance. Appl. Phys. Lett. 46, 1013-1015.

Salazar, Sánchez-Lavega A., Fernández J., 1991. Thermal diffusivity measurements in solids by the ‘‘mirage’’ technique: Experimental results. Journal of Applied Physics. 69, 1216-1223.

Zaldivar Escola F., Martínez O.E., Mingolo N., Kempf R., 2013. Photothermal microscopy applied to the characterization of nuclear fuel pellets. Journal of Nuclear Materials 435, 17–24.